
Learning to Forget for Meta-Learning

Sungyong Baik

Department of ECE, ASRI
Seoul National University
dsybaik@snu.ac.kr

Seokil Hong

Department of ECE, ASRI
Seoul National University
hongceo96@snu.ac.kr

Kyoung Mu Lee

Department of ECE, ASRI
Seoul National University
kyoungmu@snu.ac.kr

Abstract

Few-shot learning is a challenging problem where the system is required to achieve generalization from only few examples. Meta-learning tackles the problem by learning prior knowledge shared across a distribution of tasks, which is then used to quickly adapt to unseen tasks. Model-agnostic meta-learning (MAML) algorithm formulates prior knowledge as a common initialization across tasks. However, forcibly sharing an initialization brings about conflicts between tasks and thus compromises the quality of the initialization. In this work, by observing that the extent of compromise differs among tasks and between layers of a neural network, we propose a new initialization idea that employs task-dependent layer-wise attenuation, which we call selective *forgetting*. The proposed attenuation scheme dynamically controls how much of prior knowledge each layer will exploit for a given task. The experimental results demonstrate that the proposed method mitigates the conflicts and provides outstanding performance as a result. We further show that the proposed method, named L2F, can be applied and improve other state-of-the-art MAML-based frameworks, illustrating its generalizability.

1 Introduction

Recent deep learning models demonstrate outstanding performance in various fields; however, they require supervised learning with a tremendous amount of labeled data. On the other hand, humans are able to learn concepts from only few examples. Considering the cost of data annotation, the capability of humans to learn from few examples is desirable.

When there are concerns for overfitting in few-data regime, data augmentation and regularization techniques are often used. Another commonly used technique is to fine-tune a network pre-trained on large labelled data from another dataset or task [27, 34]. However, these techniques do not solve the underlying problem of few-shot learning; they fail to provide benefit when new examples are very few or too different from data used for pre-training [41]. In contrast, meta-learning tackles the problem systematically via two stages of learners; a meta-learner learns common knowledge across a distribution of tasks, which is then used for a learner to quickly learn task-specific knowledge with few examples. A popular instance is the model-agnostic meta-learning (MAML) [7], where they formulate a meta-learner to learn a common initialization that encodes the common knowledge across tasks.

The assumption of the existence of a task distribution may justify MAML for seeking a common initialization among tasks. But, there still exists variations among tasks, some of which may lead to conflict and thus compromise on the location of an initialization. Some of prior knowledge encoded in such compromised initialization is useful for one task but may be irrelevant or even detrimental for another. Consequently, a learner struggles to learn new concepts quickly with the prior knowledge that conflicts with information from new examples, which is manifested as a sharp loss landscape during optimization as shown in Figure 1(a). The sharp landscape indicates the poor generalization

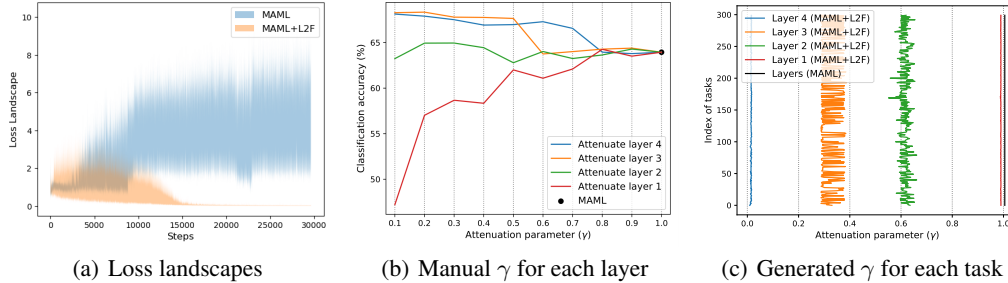


Figure 1: Loss landscapes during fast-adaptation and analysis on attenuation: (a) Loss landscapes were visualized using the methodology introduced in [31]. More details can be found in supplementary materials. MAML loss landscape (blue) becomes sharper and fluctuating as training proceeds. In contrast, L2F loss landscape (orange) becomes smoother. (b) Attenuation of an initialization by different levels (the lower γ , the stronger attenuation) for each layer affects the classification accuracy of a 4-layer CNN on miniImageNet. (c) Different attenuation parameters γ are generated by L2F for each meta-test task, especially for middle-level layers. This indicates that the amount of required prior knowledge is different for each task.

[9, 13, 23, 4, 6, 17, 31] and therefore a “bad” location of the learned initialization, as opposed to the objective of MAML.

Therefore, the catastrophic landscape sharpness signifies the necessity of reducing compromise in the initialization. One solution for a meta-learner would be to simply *forget* the compromised part of the initialization, minimizing its influence. This raises two questions: Where do these conflicts occur? To what extent? The degree of conflict varies between layers of a neural network, especially CNN, since deeper layers learn more task-specific knowledge or class-specific knowledge in classification [42]. To validate the argument, we manually attenuate the initialization with varying attenuation strength (γ) for each layer. As shown in Figure 1(b), we observe that deeper layers prefer stronger attenuation than lower layers (the lower γ , the stronger attenuation). As claimed in the previous paragraph, not only does the degree of conflict vary between layers but also between tasks, since the amount of useful information encoded in the initialization is different for each task. This is verified by different attenuation generated by our proposed method for each task. (Figure 1(c)).

We propose to facilitate selective *forgetting* by applying a task-dependent layer-wise attenuation on MAML initialization, controlling the influence of prior knowledge for each task. For task-dependency, we argue that initialization weights and its gradients (obtained from support examples of task), together, encode information about optimization specific to a task, and thus propose to condition on them to generate attenuation parameters. To achieve layer-wise attenuation, we generate an attenuation parameter for each layer. The proposed method, named L2F, indeed mitigates the compromise and improves the quality of the initialization, illustrated by a smoother landscape (as shown in Figure 1(a)) and consistent performance improvement across different domains.

2 Related Work

Meta-learning aims to learn across-task prior knowledge to achieve fast adaptation to specific tasks [2, 10, 32, 33, 37]. Recent meta-learning systems can be broadly classified into three categories: metric-based, network-based, and optimization-based. The goal of metric-based system is to learn relationship between a query and support examples by learning an embedding space, where similar classes are closer and different classes are further apart [14, 35, 36, 39]. Network-based approaches encode fast adaptation into network architecture, for example, by generating input-conditioned weights [21, 25] or employing an external memory [22, 30]. On the other hand, optimization-based systems adjust optimization for fast adaptation [7, 26, 24].

Among optimization-based systems, MAML [7] has recently received interests, owing to its simplicity and generalizability. The generalizability stems from its model-agnostic algorithm that learns across-task initialization. The initialization aims to encode prior knowledge that helps the model quickly learn and achieve good generalization performance over tasks on average. While MAML also boasts the simplicity, it shows relatively low performance on few-shot learning.

There has been several works that tried to improve the performance, especially on few-shot classification [1, 16, 18, 43, 12]. However, none of them tackles the underlying problem, which is the sharing of the starting point of adaptation to different tasks. On the contrary, LEO [29] claims that the relatively low performance comes from optimization difficulties in high-dimensional space, and proposes to generate input-dependent initializations in low-dimensional latent space. Although it achieves high performance on classification, since it uses classification-specific techniques, it is questionable whether the algorithm will exhibit the consistent performance gain in other complex problems, such as reinforcement learning. To relax the constraint on sharing the initialization, Multimodal MAML [40] transforms the MAML initialization with affine parameters. However, they do not solve the fundamental problem of the compromised prior knowledge. In fact, a general affine transformation can amplify the detrimental information, leading to poor performance and may be the reason for the lack of experiments on complex domains, such as miniImageNet classification [26].

We provide a new insight that the quality of the MAML initialization is compromised due to conflicts between tasks. This necessitates *forgetting* irrelevant or conflicting part of prior knowledge so that a learner can adapt to given tasks more easily and quickly. We argue that the amount of conflicting information present in the initialization is different for each task and each layer of a neural network. Thus, we propose to learn to *forget* the conflicting part of initialization for each task and layer by generating task-dependent layer-wise attenuation parameters, conditioned on the initialization weights and its gradients. We further demonstrate the generalizability of our method through consistent performance gain in different domains: classification, regression, and reinforcement learning.

3 Proposed Method

3.1 Problem Formulation

Before introducing the proposed method, we start with the formulation of a generic meta-learning algorithm. We assume there is a distribution of tasks $p(\mathcal{T})$, from which meta-learning algorithm aims to learn the prior knowledge, represented by a model with parameters θ . Tasks, each of which is sampled from $p(\mathcal{T})$, are split into three disjoint sets: meta-training set, meta-validation set, and meta-test set. In k -shot learning, a task \mathcal{T}_i is first sampled from the meta-training set, followed by sampling k number of examples \mathcal{D}_i from \mathcal{T}_i . These k examples are then used to quickly adapt a model with parameters, θ . Then, new examples \mathcal{D}'_i are sampled from the same task \mathcal{T}_i to evaluate the generalization performance on unseen examples with the corresponding loss function, $\mathcal{L}_{\mathcal{T}_i}$. The feedback from the loss is then used to adjust the model parameters θ to achieve better generalization. Finally, the meta-validation set is used for model selection, while the meta-test set is used for the final evaluation on the selected model.

3.2 Model-Agnostic Meta-Learning

To tackle the problem of fast adaptation to unseen tasks with few examples, we borrow the philosophy and the methodology from MAML [7]. MAML encodes prior knowledge in an initialization and seeks for a “good” common initial set of values for weights of a neural network across tasks. Formally, given a network f_θ with weights θ , MAML learns a set of initial weight values, θ , which will serve as a good starting point for fast adaptation to a new task \mathcal{T}_i , sampled from a task distribution $p(\mathcal{T})$. Given few examples \mathcal{D}_i and a loss function $\mathcal{L}_{\mathcal{T}_i}$ from the task \mathcal{T}_i , the network weights are adapted to \mathcal{T}_i during fast adaptation (or inner-loop update) as follows:

$$\theta'_i = \theta - \alpha \nabla_{\theta} \mathcal{L}_{\mathcal{T}_i}^{\mathcal{D}_i}(f_\theta). \quad (1)$$

To give feedback on the generalization performance of the model with adapted weights θ'_i to each task, the model is evaluated on new examples, \mathcal{D}'_i sampled from the same task \mathcal{T}_i . The feedback, manifested in the form of loss gradients, is used to update the initialization θ so that better generalization is achieved:

$$\theta = \theta - \eta \nabla_{\theta} \sum_{\mathcal{T}_i} \mathcal{L}_{\mathcal{T}_i}^{\mathcal{D}'_i}(f_{\theta'_i}). \quad (2)$$

3.3 Learning to Forget

Algorithm 1 Proposed Meta-Learning

Require: Task distribution $p(\mathcal{T})$

Require: Learning rates α, η

- 1: Randomly initialize θ, ϕ
 - 2: Let $\theta = \{\theta^j\}_{j=1\dots l}$ where j is the layer index and l is the number of layers of a network
 - 3: **while** not converged **do**
 - 4: Sample a batch of tasks $\mathcal{T}_i \sim p(\mathcal{T})$
 - 5: **for** each task \mathcal{T}_i **do**
 - 6: Sample examples $(\mathcal{D}, \mathcal{D}')$ from \mathcal{T}_i
 - 7: Compute $\mathcal{L}_{\mathcal{T}_i}^{\mathcal{D}}(f_\theta)$ by evaluating $\mathcal{L}_{\mathcal{T}_i}$ with respect to \mathcal{D}
 - 8: Compute attenuation parameter γ for each layer: $\{\gamma_i^j\}_{j=1\dots l} = g_\phi(\nabla_\theta \mathcal{L}_{\mathcal{T}_i}^{\mathcal{D}}(f_\theta))$,
 - 9: Compute attenuated initialization: $\bar{\theta}_i^j = \gamma_i^j \theta^j$
 - 10: Initialize $\theta'_i = \{\bar{\theta}_i^j\}_{j=1\dots l}$
 - 11: **for** number of inner-loop updates **do**
 - 12: Compute $\mathcal{L}_{\mathcal{T}_i}^{\mathcal{D}}(f_{\theta'_i})$ by evaluating $\mathcal{L}_{\mathcal{T}_i}$ with respect to \mathcal{D}
 - 13: Perform gradient descent to compute adapted weights: $\theta'_i = \theta'_i - \alpha \nabla_{\theta'_i} \mathcal{L}_{\mathcal{T}_i}^{\mathcal{D}}(f_{\theta'_i})$
 - 14: **end for**
 - 15: Compute $\mathcal{L}_{\mathcal{T}_i}^{\mathcal{D}'}(f_{\theta'_i})$ by evaluating $\mathcal{L}_{\mathcal{T}_i}$ with respect to \mathcal{D}'
 - 16: **end for**
 - 17: Perform gradient descent to update weights: $(\theta, \phi) \leftarrow (\theta, \phi) - \eta \nabla_{(\theta, \phi)} \sum_{\mathcal{T}_i} \mathcal{L}_{\mathcal{T}_i}^{\mathcal{D}'}(f_{\theta'_i})$
 - 18: **end while**
-

While MAML is elegantly simple, its limitation comes from the very fact that the initialization is shared across a distribution of tasks. On the contrary to the goal of MAML, which is to learn a “good” starting point for fast adaptation to new tasks, the shared initialization, in fact, hinders the fast learning process, as illustrated in Figure 1(a). This is mainly due to disagreement between tasks on the location of a “good” starting point. The forcibly shared initialization does not resolve the conflicts but is rather compromised. As a result, the learner finds some part of the initialization to be irrelevant or even detrimental for learning a given task. We thus propose to discard such compromised part of the prior knowledge via attenuating the initialization parameters θ directly. Then, one may ask which parameter is compromised? To answer the question, we refer to the previous finding that lower layers of a CNN encode general knowledge while deeper layers contain more task-specific information [42]. Upon this observation, we hypothesize that low-level layers do not need much attenuation while high-level layers do. To support our hypothesis, we perform an experiment, shown in Figure 1(b), where we vary the amount of attenuation (γ^j) on each layer to observe how much each layer benefits. As expected, high-level layers favor stronger attenuation while lower layers prefer little to no attenuation. This leads to the second question: How much should the parameters be attenuated layer-wise? One answer would be to let a model learn to find an optimal set of attenuations. The answers to these two questions lead to our proposal: learn layer-wise attenuation via applying a learnable parameter γ^j on the initialization parameter of each layer θ^j as follows:

$$\bar{\theta}^j = \gamma^j \theta^j, \quad (3)$$

where j is the layer index of a neural network. The attenuated initialization $\bar{\theta}$ serves as a new starting point for fast adaptation to tasks. Although this may reduce the extent of compromise that may exist in the original MAML initialization, one may ask if the amount of unnecessary or contradicting information in the initialization is equal across tasks. Surely, the degree of agreement and disagreement with others differs for different tasks. This can be observed in Figure 1(b), where the classification accuracy fluctuates as attenuation strength varies for layer 2 of a network. This is because there is no consensus between tasks on what the best attenuation is for layer 2, as further indicated by different attenuation preferred by each task in Figure 1(c). To resolve such conflict, in addition to the layer-wise attenuation, we propose a task-dependent attenuation. But, this poses another question: What information can be used to make attenuation task-dependent? We turn to gradients $\nabla_\theta \mathcal{L}_{\mathcal{T}_i}^{\mathcal{D}}(f_\theta)$ for the answer. Gradients, used for fast adaptation via gradient descents, not only hold task-specific information but also encode the quality of the initialization with respect to the given task \mathcal{T}_i from the perspective of optimization. Thus, we propose to compute gradient $\nabla_\theta \mathcal{L}_{\mathcal{T}_i}^{\mathcal{D}}(f_\theta)$ at the initialization and condition a network g_ϕ on it to generate the task-dependent attenuation:

$$\gamma_i = g_\phi(\nabla_\theta \mathcal{L}_{\mathcal{T}_i}^{\mathcal{D}}(f_\theta)), \quad (4)$$

where $\gamma_i = \{\gamma_i^j\}$ is the set of layer-wise gammas for the i -th task and g_ϕ is a 3-layer MLP network of parameters ϕ , with a sigmoid at the end to facilitate attenuation. For the network g_ϕ to generate layer-wise gammas, the network is conditioned on layer-wise mean of gradients.

After the initialization is adapted to each task, the network undergoes fast adaptation as in Equation 1 and the initialization is updated as in Equation 2 during training. The overall training procedure is summarized in Algorithm 1.

4 Experiments

In this section, we demonstrate the effectiveness and generalizability of our method through extensive experiments on various problems, including few-shot classification, regression, and reinforcement learning.

4.1 Few-Shot Classification

Two well-known datasets are used for classification problem, both of which are extracted from ImageNet dataset while taking into account for few-learning scenarios. Specifically, one of the subsets, miniImageNet is constructed by randomly selecting 100 classes from the ILSVRC-12 dataset, with each class consisting of 600 images of size 84×84 [39]. The constructed dataset is divided into 3 disjoint subsets: 64 classes for training, 16 for validation, and 20 for test as in [26].

tieredImageNet is a larger subset with 608 classes with 779,165 images of size 84×84 in total. Classes are grouped into 34 categories, according to ImageNet hierarchy. These categories are then split into 3 disjoint sets: 20 categories for training, 6 for validation, and 8 for test. According to [28], this minimizes class similarity between training and test and thus makes the problem more challenging and realistic.

Experiments are conducted under typical settings: 5-way 1-shot and 5-way 5-shot classification. Following many recent few-shot classification systems, we utilize ResNet12 from [25] as a backbone.

4.1.1 Results

The results of our proposed approach, other baselines and existing state-of-the-art approaches on the miniImageNet and tieredImageNet are presented in Table 1 and Table 2, respectively. The

Table 1: Test accuracy on 5-way miniImageNet classification

	Backbone	miniImageNet	
		1-shot	5-shot
Matching Network [39]	4 conv	$43.44 \pm 0.77\%$	$55.31 \pm 0.73\%$
Meta-Learner LSTM [26]	4 conv	$43.56 \pm 0.84\%$	$60.60 \pm 0.71\%$
MetaNet [21]	5 conv	$49.21 \pm 0.96\%$	—
LLAMA [8]	4 conv	$49.40 \pm 0.84\%$	—
Relation Network [36]	4 conv	$50.44 \pm 0.82\%$	$65.32 \pm 0.70\%$
Prototypical Network [35]	4 conv	$49.42 \pm 0.78\%$	$68.20 \pm 0.66\%$
MAML [7]	4 conv	$48.70 \pm 1.75\%$	$63.11 \pm 0.91\%$
MAML++ [1]	4 conv	$52.15 \pm 0.26\%$	$68.32 \pm 0.44\%$
MAML+L2F (Ours)	4 conv	$52.10 \pm 0.50\%$	$69.38 \pm 0.46\%$
MetaGAN [43]	ResNet12	$52.71 \pm 0.64\%$	$68.63 \pm 0.67\%$
SNAIL [20]	ResNet12 (pre-trained)	$55.71 \pm 0.99\%$	$68.88 \pm 0.92\%$
adaResNet [22]	ResNet12	$56.88 \pm 0.62\%$	$71.94 \pm 0.57\%$
CAML [12]	ResNet12 (pre-trained)	$59.23 \pm 0.99\%$	$72.35 \pm 0.71\%$
TADAM [25]	ResNet12 (pre-trained)	$58.5 \pm 0.3\%$	$76.7 \pm 0.3\%$
MAML	ResNet12	$51.03 \pm 0.50\%$	$68.26 \pm 0.47\%$
MAML+L2F (Ours)	ResNet12	$57.48 \pm 0.49\%$	$74.68 \pm 0.43\%$
LEO [29]	WideResNet34 (pre-trained)	$61.76 \pm 0.08\%$	$77.59 \pm 0.12\%$
LEO (reproduced)	WideResNet34 (pre-trained)	$61.50 \pm 0.17\%$	$77.12 \pm 0.07\%$
LEO+L2F (Ours)	WideResNet34 (pre-trained)	$62.12 \pm 0.13\%$	$78.13 \pm 0.15\%$

Table 2: Test accuracy on 5-way tieredImageNet classification

	Backbone	tieredImageNet	
		1-shot	5-shot
MAML	4 conv	49.06 \pm 0.50%	67.48 \pm 0.47%
MAML+L2F (Ours)	4 conv	54.40 \pm 0.50%	73.34 \pm 0.44%
MAML	ResNet12	58.58 \pm 0.49%	71.24 \pm 0.43%
MAML+L2F (Ours)	ResNet12	63.94 \pm 0.48%	77.61 \pm 0.41%
LEO	WideResNet34 (pre-trained)	66.33 \pm 0.05%	81.44 \pm 0.09%
LEO (reproduced)	WideResNet34 (pre-trained)	67.02 \pm 0.11%	82.29 \pm 0.16%
LEO+L2F (Ours)	WideResNet34 (pre-trained)	68.00 \pm 0.11%	83.02 \pm 0.08%

proposed method improves MAML by a large margin. We note that our proposed approach remains model-agnostic and achieves better or comparable accuracy to state-of-the-art approaches with the same backbone, without using any classification-specific techniques, such as fine-tuning. To show generalization of the contribution, we apply L2F to the state-of-the-art MAML-based system LEO and demonstrate the performance improvement, achieving the new state-of-the-art performance.

4.1.2 Ablation Studies

Inner-loop update steps One may argue that the comparisons are not fair because there is one extra adjustment to initialization parameters before inner-loop updates. Table 3 shows ablation studies on the number of inner-loop updates for the proposed and the baseline to demonstrate that the performance gain is not due to an extra number of adjustments to parameters. Rather, the benefits come from *forgetting* the unnecessary information, helping the learner quickly adapt to new tasks.

Table 3: Ablation studies on inner-loop update steps on 5-way 5-shot miniImageNet classification.

Inner-loop update steps	MAML	MAML+L2F (Ours)
1	56.93 \pm 0.32%	68.16 \pm 0.47%
2	55.63 \pm 0.50%	66.85 \pm 0.49%
3	58.79 \pm 0.49%	68.61 \pm 0.46%
4	62.72 \pm 0.45%	68.66 \pm 0.43%
5	63.94 \pm 0.41%	69.38 \pm 0.46%
6	64.54 \pm 0.46%	—

Attenuation Type One may be curious and ask: Is layer-wise attenuation the best way to go? Thus, we analyze different types of attenuation; a single attenuation parameter for the whole network, or an individual attenuation parameter for each layer, each filter, and each weight of the network. To focus on investigating which type of attenuation is the most beneficial, we remove the task-dependent part and make the attenuation parameters learnable (with values initialized to be 1), rather than generated.

We perform an ablation study with a 4-layer CNN in 5-way 5-shot classification setting on mini-ImageNet and present results in Table 4. As expected, the layer-wise attenuation gave the most performance gain. Weight-wise or filter-wise attenuation parameter may have finer control, but these parameters have limited scope in that they do not have information about conflicts that occur at the

Table 4: Ablation studies on attenuation

Attenuation Type	Accuracy
None (MAML, our reproduction)	63.94 \pm 0.48%
parameter-wise	64.7 \pm 0.43%
filter-wise	65.35 \pm 0.48%
layer-wise	68.49 \pm 0.41%
network-wise	67.84 \pm 0.46%
MAML+L2F (Ours)	69.38 \pm 0.46%

Table 5: Ablation studies on task-dependent transformation

Model	Description	Accuracy
1	MAML (our reproduction)	63.94 \pm 0.48%
2	MAML + task-dependent non-sigmoided γ_i^j, β_i^j	66.22 \pm 0.47%
3	MAML + task-dependent non-sigmoided γ_i^j	67.56 \pm 0.47%
Ours	MAML + L2F (task-dependent sigmoided γ_i^j)	69.38 \pm 0.46%

level of layers or network. On the other hand, layer-wise and network-wise parameters gain information about conflicts in neighbor weights as gradients pass through different weights/filters to reach the same attenuation parameter, since the attenuation parameter is shared by these weights/filters.

Task-Dependent Transformation Type To analyze how much performance gain comes from each part of L2F (i.e. *forgetting* and task-dependency), we apply each module separately to MAML and present results in Table 5. Since the investigation on effectiveness of attenuation has already been presented in Table 4, we now focus on the effectiveness of the task-dependent transformation to study if there are benefits of transforming initialization in general. To that end, we explore different types of task-dependent transformations of the initialization. We start with the simple superset of the attenuation: γ without sigmoid (Model 3) such that γ_i is no longer restricted to be between 0 and 1, and hence does not facilitate attenuation. We also explore a more flexible option: affine transformation (Model 2), where the network g_ϕ generates two sets of parameters γ_i, β_i without sigmoid, which will modulate f_θ via $\gamma_i^j \theta^j + \beta_i^j$.

Table 5 illustrates that MAML gains performance boost throughout different types of task-dependent transformation, suggesting the benefits of the task-dependency. It is reasonable to expect that more flexibility of transformation (Model 2 and 3) would allow for tasks to bring the initialization to more appropriate location for fast adaptation. Interestingly, the classification accuracy drops as more flexibility is given to the transformation of the initialization. This seeming contradiction underlines the necessity of attenuation (sigmoided γ_i^j in our model), rather than just naïve transformation, of the initialization to *forget* the compromised part of the prior knowledge encoded in the initialization.

4.2 Regression

We investigate the generalizability of the proposed method across domains, starting with evaluating the performance in k -shot regression. In k -shot regression, the objective is to fit a function, given k samples of points. Following the general settings in [7, 18], the target function is set to be a sinusoid with varying amplitude and phase between tasks. The sampling range of amplitude, frequency, and phase defines a task distribution and is set to be the same for both training and evaluation. Regression is visualized in Figure 2(a), while its prediction, measured in mean-square error (MSE), is presented in Table 6. The results demonstrate that our method not only converges faster but also fits to target functions more accurately.

To further stress the generalization of the MAML+L2F initialization, we extensively increase the degree of conflicts between new tasks and the prior knowledge. To that end, we modify the setting such that amplitude, frequency, and phase are sampled from the non-overlapped ranges for training and evaluation (please refer to the supplementary material for details). In Figure 2(b), our model exhibits higher accuracy and thus claims the better generalization.

Table 6: MSE averaged over the sampled 100 points with 95% confidence intervals on k -shot regression. Our method consistently outperforms across all gradient steps.

	Models	1 step	2 steps	5 steps
5-shot training	MAML	1.2247	1.0268	0.8995
	MAML+L2F (Ours)	1.0537	0.8426	0.7096
10-shot training	MAML	0.9884	0.6192	0.4072
	MAML+L2F (Ours)	0.8069	0.5317	0.3696
20-shot training	MAML	0.6144	0.3346	0.1817
	MAML+L2F (Ours)	0.5475	0.2805	0.1629

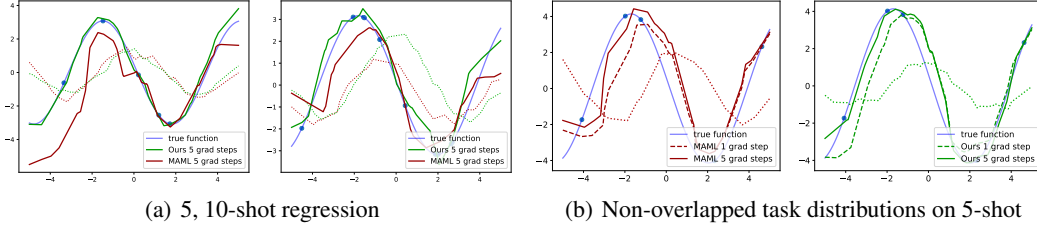


Figure 2: MAML + L2F (Ours) vs MAML on Few-shot regression: (a) Tasks are sampled from the same distribution for training and evaluation. (b) Tasks are sampled from the non-overlapped distributions for training and evaluation. In both cases, MAML+L2F (Ours) is more fitted to the true function.

4.3 Reinforcement Learning

To further validate the generalizability of L2F, we evaluate the performance in reinforcement learning, specifically in 2D navigation and locomotion environments from [5] as in [7]. We briefly outline the task description below (please refer to the supplementary material for details). Figure 3 presents consistent improvement over MAML across different experiments. This solidifies the generalizability and effectiveness of our proposed method.

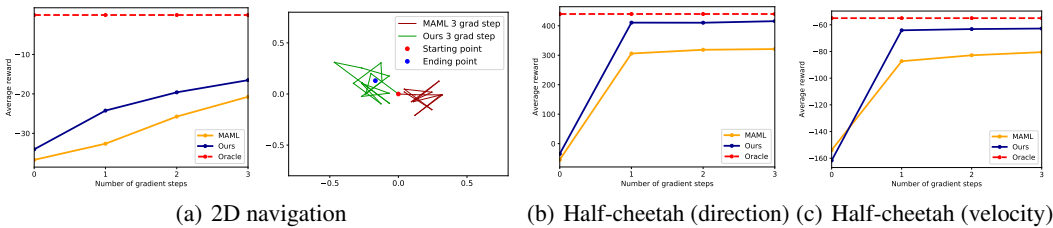


Figure 3: Reinforcement learning results for 3 different environments. The results show that MAML+L2F(Ours) can adapt to each task substantially faster than MAML.

4.3.1 2D Navigation

A 2D navigation task is to move an agent from the starting point to the destination point in 2D space, where the reward is defined as the negative of the squared distance to the destination point. We follow the experiment procedure from [7], where they fix the starting point and only vary the location of destination between tasks.

Figure 3(a) presents faster and more precise navigation by our model in both experiment settings, both quantitatively and qualitatively. This solidifies the severity of the conflicts between tasks.

4.3.2 Mujoco

As a more complex reinforcement-learning environment, we experiment on locomotion with the MuJoCo simulator [38], where there are two sets of tasks: a robot is required to move in a particular direction in one set and move with a particular velocity in the other. For both experiments, our method outperforms MAML in large margins as shown in Figure 3(b).

5 Conclusion

In this paper, we argue that forcibly sharing a common initialization in MAML induces conflicts across tasks and thus results in compromised quality of the initialization. The severe sharpness of the loss landscape asserts that such compromise makes the MAML initialization a “bad” starting position for fast adaptation, rather than a “good” starting position, which is the original goal of MAML. We propose to resolve this discrepancy by facilitating *forgetting* of the irrelevant information that may hinder fast adaptation. Specifically, we propose a task-dependent layer-wise attenuation, named L2F, from the observation that the degree of compromise varies between network layers and tasks. Through extensive experiments across different domains, we validate our argument that the compromise present in the initialization is critical and is greatly resolved by selective *forgetting*.

References

- [1] A. Antoniou, H. Edwards, and A. Storkey. How to train your maml. In *ICLR*, 2019.
- [2] S. Bengio, Y. Bengio, J. Cloutier, and J. Gecsei. On the optimization of a synaptic learning rule. In *Preprints Conf. Optimality in Artificial and Biological Neural Networks*, pages 6–8. Univ. of Texas, 1992.
- [3] L. Bertinetto, J. F. Henriques, P. Torr, and A. Vedaldi. Meta-learning with differentiable closed-form solvers. In *ICLR*, 2019.
- [4] P. Chaudhari, A. Choromanska, S. Soatto, Y. LeCun, C. Baldassi, C. Borgs, J. Chayes, L. Sagun, and R. Zecchina. Entropy-sgd: Biasing gradient descent into wide valleys. In *ICLR*, 2017.
- [5] Y. Duan, X. Chen, S. J. Houthoofd, Rein, and P. Abbeel. Benchmarking deep reinforcement learning for continuous control. In *ICML*, 2016.
- [6] G. K. Dziugaite and D. M. Roy. Computing nonvacuous generalization bounds for deep(stochastic) neural networks with many more parameters than training data. In *UAI*, 2017.
- [7] C. Finn, P. Abbeel, and S. Levine. Model-agnostic meta-learning for fast adaptation of deep networks. In *ICML*, 2017.
- [8] E. Grant, C. Finn, S. Levine, T. Darrell, and T. Griffiths. Recasting gradient-based meta-learning as hierarchical bayes. In *ICLR*, 2018.
- [9] S. Hochreiter and J. Schmidhuber. Flat minima. *Neural computation*, 9(1):1–42, 1997.
- [10] S. Hochreiter, A. Younger, and P. Conwell. Learning to learn using gradient descent. *Artificial Neural Networks, ICANN 2001*, pages 87–94, 2001.
- [11] S. Ioffe and C. Szegedy. Batch normalization: Accelerating deep network training by reducing internal covariate shift. In *ICML*, 2015.
- [12] X. Jiang, M. Havaei, F. Varno, G. Chartrand, N. Chapados, and S. Matwin. Learning to learn with conditional class dependencies. In *ICLR*, 2019.
- [13] N. S. Keskar, D. Mudigere, J. Nocedal, M. Smelyanskiy, and P. T. P. Tang. On large-batch training for deep learning: Generalization gap and sharp minima. In *ICLR*, 2017.
- [14] G. Koch, R. Zemel, and R. Salakhutdinov. Siamese neural networks for one-shot image recognition. In *ICML Deep Learning Workshop*, 2015.
- [15] A. Krizhevsky and G. Hinton. Learning multiple layers of features from tiny images. University of Toronto.
- [16] Y. Lee and S. Choi. Gradient-based meta-learning with learned layerwise metric and subspace. In *ICML*, 2018.
- [17] H. Li, Z. Xu, G. Taylor, C. Studer, and T. Goldstein. Visualizing the loss landscape of neural nets. In *NIPS*, 2018.
- [18] Z. Li, F. Zhou, F. Chen, and H. Li. Meta-sgd: Learning to learn quickly for few shot learning. *CoRR*, abs/1707.09835, 2017.
- [19] Y. Liu, J. Lee, M. Park, S. Kim, E. Yang, S. J. Hwang, and Y. Yang. Learning to propagate labels: Transductive propagation network for few-shot learning. In *ICLR*, 2019.
- [20] N. Mishra, M. Rohaninejad, X. Chen, and P. Abbeel. A simple neural attentive meta-learner. In *ICLR*, 2018.
- [21] T. Munkhdalai and H. Yu. Meta networks. In *ICML*, 2017.
- [22] T. Munkhdalai, X. Yuan, S. Mehri, and A. Trischler. Rapid adaptation with conditionally shifted neurons. In *ICML*, 2018.
- [23] B. Neyshabur, S. Bhojanapalli, D. McAllester, and N. Srebro. Exploring generalization in deep learning. In *NIPS*, 2017.
- [24] A. Nichol, J. Achiam, and J. Schulman. On first-order meta-learning algorithms. *CoRR*, abs/1803.02999, 2018.
- [25] B. N. Oreshkin, P. Rodriguez, and A. Lacoste. Tadam: Task dependent adaptive metric for improved few-shot learning. In *NIPS*, 2018.

- [26] S. Ravi and H. Larochelle. Optimization as a model for few-shot learning. In *ICLR*, 2017.
- [27] A. S. Razavian, H. Azizpour, J. Sullivan, and S. Carlsson. Cnn features off-the-shelf: an astounding baseline for recognition. In *CVPR Workshop*, 2014.
- [28] M. Ren, E. Triantafillou, S. Ravi, J. Snell, K. Swersky, J. B. Tenenbaum, H. Larochelle, and R. S. Zemel. Meta-learning for semi-supervised few-shot classification. In *ICLR*, 2018.
- [29] A. A. Rusu, D. Rao, J. Sygnowski, O. Vinyals, R. Pascanu, S. Osindero, and R. Hadsell. Meta-learning with latent embedding optimization. In *ICLR*, 2019.
- [30] A. Santoro, S. Bartunov, M. Botvinick, D. Wierstra, and T. Lillicrap. Meta-learning with memory-augmented neural networks. In *ICLR*, 2016.
- [31] S. Santurkar, D. Tsipras, A. Ilyas, and A. Madry. How does batch normalization help optimization? In *NIPS*, 2018.
- [32] J. Schmidhuber. Evolutionary principles in self-referential learning. *On learning how to learn: The meta-meta-... hook.*) *Diploma thesis, Institut f. Informatik, Tech. Univ. Munich*, 1987.
- [33] J. Schmidhuber. Learning to control fast-weight memories: An alternative to dynamic recurrent networks. *Neural Computation*, 4(1):131–139, 1992.
- [34] K. Simonyan and A. Zisserman. Very deep convolutional networks for large-scale image recognition. In *ICLR*, 2015.
- [35] J. Snell, K. Swersky, and R. Zemel. Prototypical networks for few-shot learning. In *NIPS*, 2017.
- [36] F. Sung, Y. Yang, L. Zhang, T. Xiang, P. H. Torr, and T. M. Hospedales. Learning to compare: Relation network for few-shot learning. In *CVPR*, 2018.
- [37] S. Thrun and L. Pratt. *Learning to learn*. Springer Science & Business Media, 2012.
- [38] E. Todorov, T. Erez, and Y. Tassa. Mujoco: A physics engine for model-based control. In *IROS*, 2012.
- [39] O. Vinyals, C. Blundell, T. Lillicrap, k. kavukcuoglu, and D. Wierstra. Matching networks for one shot learning. In *NIPS*, 2016.
- [40] R. Vuorio, S.-H. Sun, H. Hu, and J. J. Lim. Toward multimodal model-agnostic meta-learning. In *NIPS Meta-Learning Workshop*, 2018.
- [41] J. Yosinski, J. Clune, Y. Bengio, and H. Lipson. How transferable are features in deep neural networks? In *NIPS*, 2014.
- [42] M. D. Zeiler and R. Fergus. Visualizing and understanding convolutional networks. In *ECCV*, 2014.
- [43] R. Zhang, T. Che, Z. Ghahramani, Y. Bengio, and Y. Song. Metagan: An adversarial approach to few-shot learning. In *NIPS*, 2018.

A Extended Experiments on Classification

To further validate that our method consistently provides benefits regardless of scenarios, we compare our method against the baseline on additional datasets that have been recently introduced: FC100 (Fewshot-CIFAR100) [25] and CIFAR-FS (CIFAR100 few-shots) [3]. Both aim for creating more challenging scenarios by using low resolution images (32×32 , compared to 84×84 in miniImageNet [26] and tieredImageNet [28]) from CIFAR100 [15]. These two datasets differ in how they create the train/val/test splits of CIFAR100. While CIFAR-FS follows the procedure that was used for miniImageNet, FC100 aligns more with the goal of tieredImageNet in that they try to minimize the amount overlap between splits by splitting based on superclasses. Table G presents results for FC100 and Table H for CIFAR-FS.

Table G: Test accuracy on FC100 5-way classification

	Backbone	FC100		
		1-shot	5-shot	10-shot
MAML (our reproduction)	4 conv	$35.98 \pm 0.48\%$	$51.40 \pm 0.50\%$	$56.13 \pm 0.50\%$
MAML+L2F (Ours)	4 conv	$39.46 \pm 0.49\%$	$53.12 \pm 0.50\%$	$59.72 \pm 0.49\%$

Table H: Test accuracy on CIFAR-FS 5-way classification

	Backbone	CIFAR-FS	
		1-shot	5-shot
MAML (Our reproduction)	4 conv	$53.91 \pm 0.50\%$	$70.16 \pm 0.46\%$
MAML+L2F (Ours)	4 conv	$57.28 \pm 0.49\%$	$73.94 \pm 0.44\%$

B Loss Landscape

In [31], they analyze the stability and smoothness of the optimization landscape by measuring Lipschitzness and the “effective” β -smoothness of loss. We use these measurements to analyze learning dynamics for both MAML and our proposed method during training on 5-way 5-shot miniImageNet classification tasks. In Figure D, we start with investigating fast-adaptation (or inner-loop) optimization. At each inner-loop update step, we measure variations in loss (Figure D (a)), the l_2 difference in gradients (Figure D (b)), and the maximum difference in gradient over the distance (Figure D (c)), as we move to different points along the computed gradient for that gradient descent. We take an average of these values over the number of inner-loop updates and plot them against training iterations. With a similar approach, we also analyze the optimization stability of fast adaptation to validation tasks at every epoch (Figure E). The measurements were averaged over (the number of validation tasks \times the number of inner-loop update steps).

At the initial stages of training, L2F appears to struggle more, while optimization of MAML seems more stable. This may seem contradictory at first but this actually validates our argument about conflicts between tasks even further. At the beginning, the MAML initialization is not trained enough and thus does not have sufficient prior knowledge of task distribution yet. As training proceeds, the initialization encodes more information about task distribution and encounters conflicts between tasks more frequently.

As for L2F, the attenuator network g_ϕ initially does not have enough knowledge about the task distribution and thus generates meaningless attenuation γ , deteriorating the initialization. But, the attenuator network increasingly encodes more information about the task distribution, generating more appropriate attenuation γ that corresponds to tasks well. The generated γ accordingly allows for a learner to *forget* the irrelevant part of prior knowledge to help fast adaptation, as illustrated by increasing stability and smoothness of landscape in Figure D. The similar observation can be made from E, illustrating the generalizability and the robustness of the proposed method to unseen tasks.

We also investigate the optimization landscape of learning the initialization θ itself for both MAML and L2F in Figure F. The figure demonstrates that the more stable and smoother landscape is realized by L2F. Because the task-dependent layer-wise attenuation allows for *forgetting* the irrelevant or

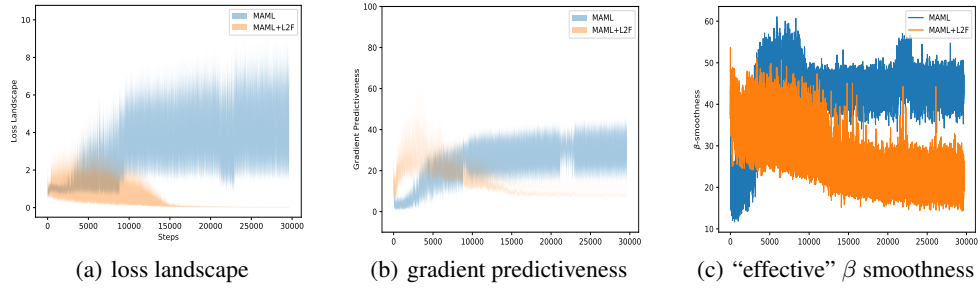


Figure D: Analysis of the optimization landscape of the fast adaptation to tasks from the meta-training set. In each subfigure, averaged values are shown for each training iteration.

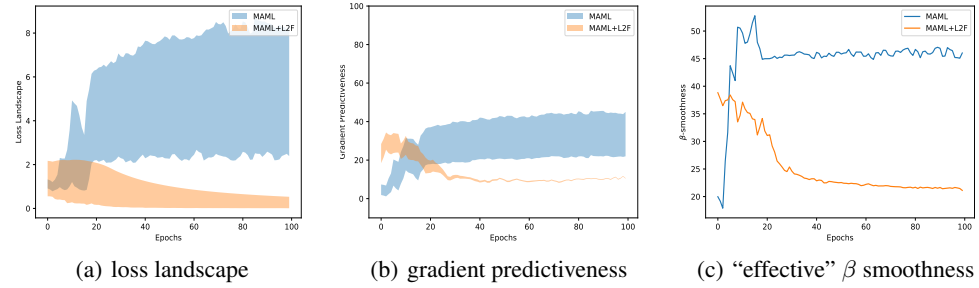


Figure E: Analysis of the optimization landscape of the fast adaptation to tasks from the meta-validation set. In each subfigure, averaged values are shown for each training epoch.

conflicting part of prior knowledge present in the initialization θ , it lifts a burden of trying to resolve conflicts between tasks from θ , allowing for more stable training of the initialization itself.

C Regression

C.1 Additional Qualitative results

In Figure G and H, we show a random sample of qualitative results from the k -shot sinusoid regression, where $k \in [5, 10]$. The target function (or true function) is a sine curve $y(x) = A \sin(\omega x + b)$ with the amplitude A , frequency ω , phase b , and the input range $[-5.0, 5.0]$. The sampling range of amplitude, frequency, and phase defines a task distribution. In Figure G, we follow the general settings in [7, 18], where amplitude A , frequency ω , and phase b are sampled from the uniform distribution on intervals $[0.1, 5.0]$, $[0.8, 1.2]$, and $[0, \pi]$, respectively. MAML+L2F demonstrates more accurate regression for both 5 and 10-shot cases, compared to the baseline, MAML. To further stress the generalization of the MAML+L2F initialization, we extensively increase the degree of conflicts between new tasks and

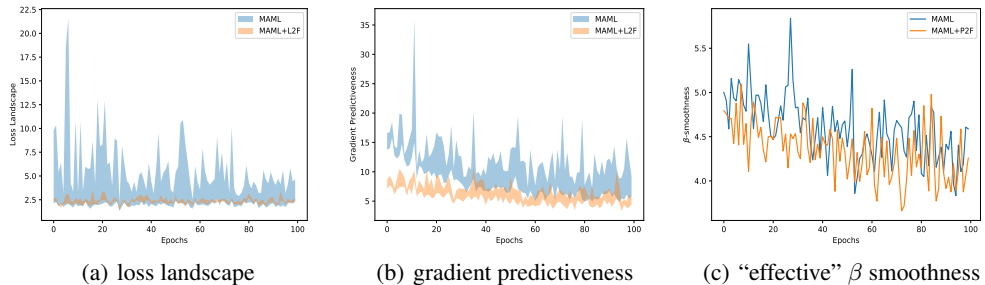


Figure F: Analysis of the optimization landscape of the initialization learning dynamics.

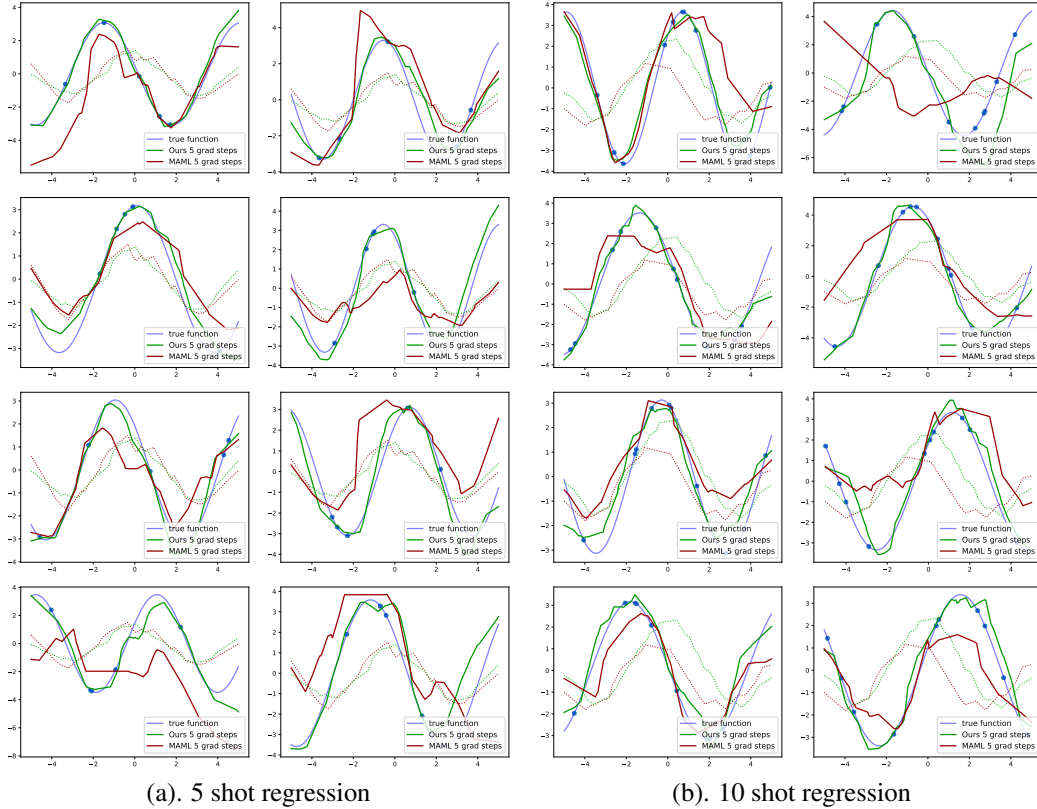


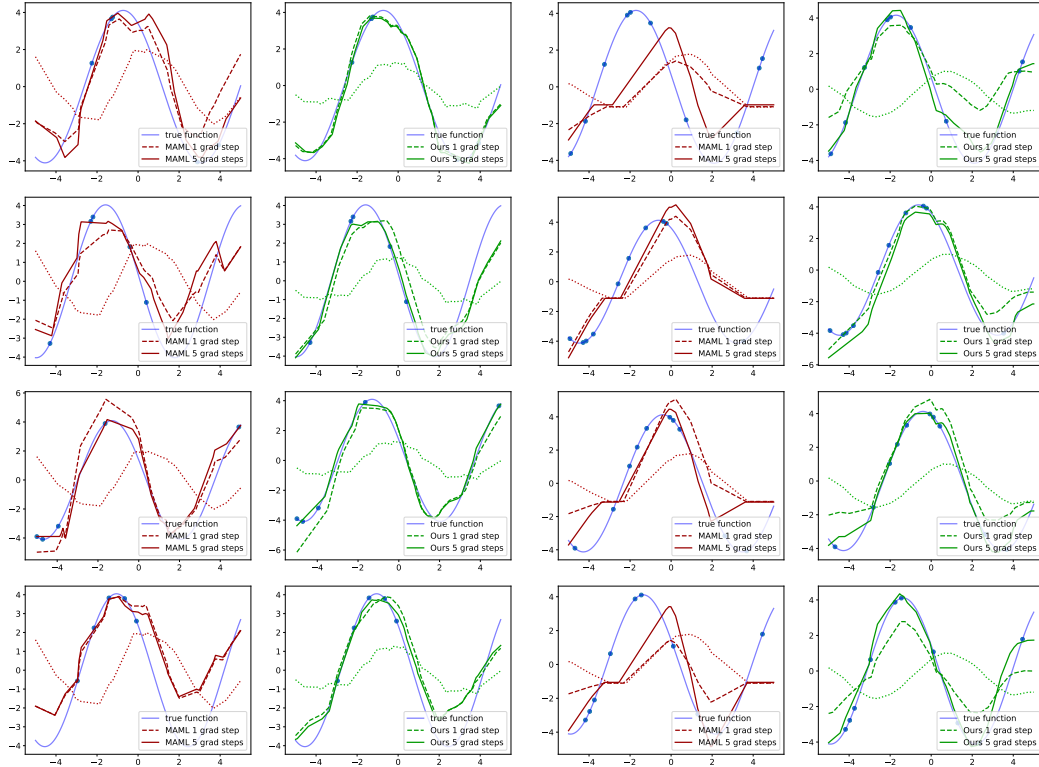
Figure G: Qualitative results for the k -shot sinusoid regression ($y(x) = A\sin(\omega x + b)$), where $k \in [5, 10]$. Parameters are sampled from the same distribution for training and evaluation.

the prior knowledge. To that end, we modify the setting such that amplitude, frequency, and phase are sampled from the non-overlapped ranges for training and evaluation. In training, amplitude A , frequency ω , and phase b are sampled from the uniform distribution on intervals $[0.1, 3.0]$, $[0.8, 1.0]$, and $[0, \pi/2]$, respectively. In evaluation, amplitude A , frequency ω , and phase b are sampled from the uniform distribution on intervals $[3.0, 5.0]$, $[1.0, 1.2]$, and $[\pi/2, \pi]$, respectively. In Figure H, our method(MAML+L2F) exhibits better fitting and thus claims the better generalization than MAML for both 5 and 10-shot regression.

D Reinforcement Learning

D.1 Additional Qualitative results

The qualitative results for the 2D navigation experiments are shown in Figure I. In training, the position of starting point is fixed at $[0, 0]$ and the position of destination is randomly sampled from space $[-0.5 \times 0.5, -0.5 \times 0.5]$, which is the same experiment procedure from [7]. Velocity is clipped to be in the range $[-0.2, 0.2]$. In evaluation, we performed experiments with four different task distributions. In Figure I(a), the task distribution for evaluation is the same as for training. On the other hand, as in regression experiment H, we perform additional 3 experiments (Figure I(b),I(c),I(d)) that evaluate models under extreme conditions, where the task distribution for evaluation is chosen to be different from the task distribution for training. In Figure I(b), the starting point is no longer fixed but rather sampled from space $[-0.5 \times 0.5, -0.5 \times 0.5]$. In Figure I(c), the position of starting point is fixed at $[0, 0]$. However, the position of the ending point is sampled from a larger space $[-2.0 \times 2.0, -2.0 \times 2.0]$. In Figure I(d), both the starting and destination positions are sampled from space $[-2.0 \times 2.0, -2.0 \times 2.0]$. Overall, our proposed method demonstrates more accurate and robust navigation, compared to the baseline MAML.



(a). Non-overlapped task distributions on 5-shot (b). Non-overlapped task distributions on 10-shot

Figure H: Qualitative results for the k -shot sinusoid regression ($y(x) = A \sin(\omega x + b)$), where $k \in [5, 10]$. Parameters are sampled from non-overlapped ranges for training and evaluation.

E Implementation Details

E.1 classification

E.1.1 Experiment Setup

We use the standard settings [7] for N -way k -shot classification in both miniImageNet[26] and tieredImageNet[28]. When calculating gradients for fast adaptation to each task, the number of examples \mathcal{D} used is either N . The fast adaptation is done via 5 gradient steps with the fixed step size, $\alpha = 0.01$ for all models, except LEO and LEO+L2F during both training and evaluation. Gradients for meta-updating the networks f_θ and g_ϕ are calculated with 15 number of examples \mathcal{D}' at each iteration. The MAML and its variants were trained for 50000 iterations in miniImageNet and 125000 in tieredImageNet to account for the larger number of examples as in [19]. The meta batch size of tasks is set to be 2 for 5-shot and 4 for 1-shot, with the exception that the batch size is 1 for ResNet12 in miniImageNet and tieredImageNet. This is due to the limited memory and the heavy computation load from the combination of second-order gradient computation, large image size, and a larger network.

As for experiments with LEO, we follow the exact setup from LEO [29]. We only add attenuation process before adaptation in latent space and fine-tuning in parameter space for LEO+L2F.

E.1.2 Network Architecture for f_θ

4 conv As with most algorithms [39, 26, 35, 36] that use 4-layer CNN as a backbone, we use 4 layers each of which contains 64-filter 3×3 convolution filters, a batch normalization [11], a Leaky ReLU nonlinearity, and a 2×2 max pooling. Lastly, the classification linear layer and softmax are placed at the end of the network.

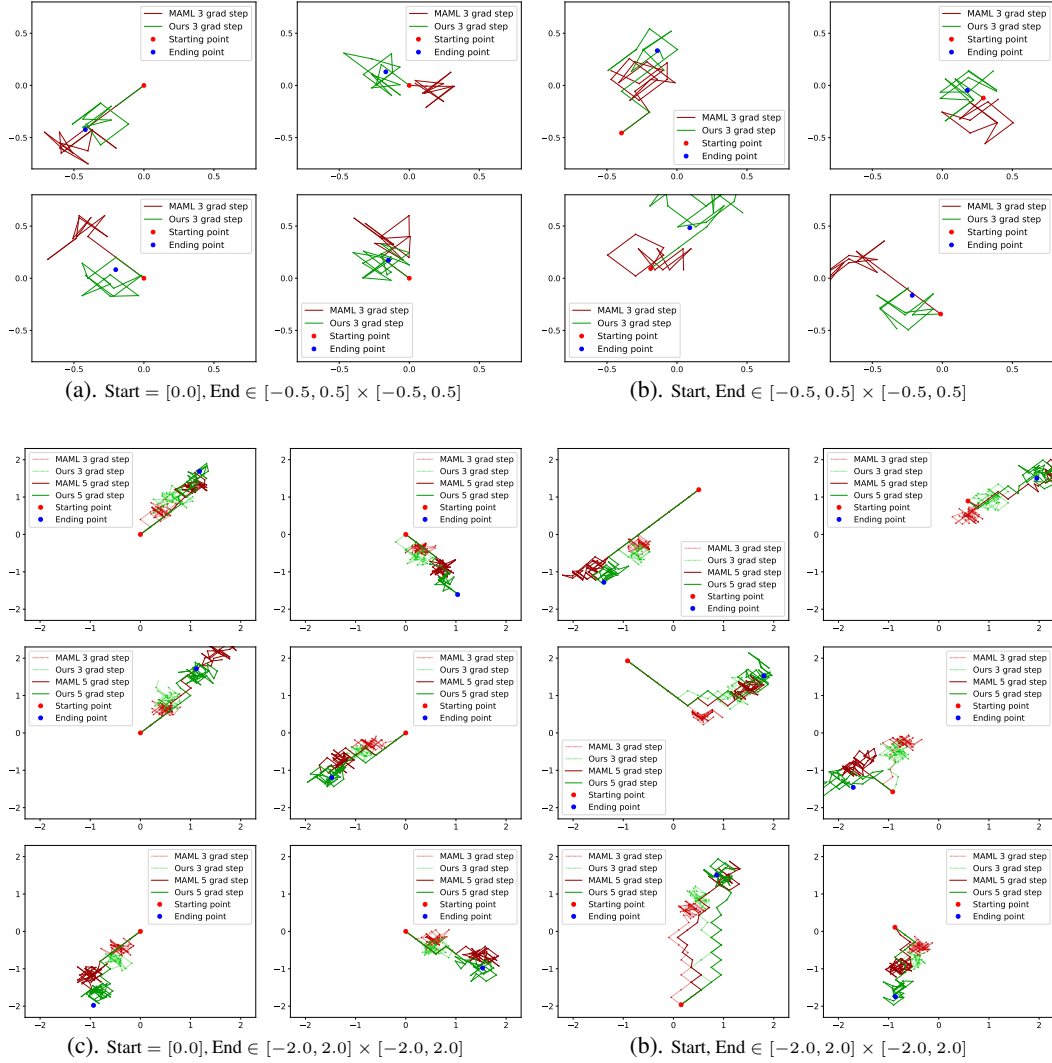


Figure I: Qualitative results for the 2D Navigation task with MAML vs MAML+L2F (Ours) comparison. Only (a) experiment, tasks are sampled from the same distribution for training and evaluation, and (b), (c), and (d) experiments, tasks are sampled from the non-overlapped ranges for training and evaluation

ResNet12 As for the ResNet12 architecture, the network consists of 4 residual blocks. each residual block consists of three 3×3 convolution layers. The first two convolution layers are followed by a batch normalization and a Leaky ReLU nonlinearity. The last convolution layer is followed by a batch normalization and a skip connection that contains a 1×1 convolution layer and a batch normalization. After a skip connection, a Leaky ReLU nonlinearity and a max 2×2 are placed at the end of each residual block.

The number of convolution filters for 4 residual blocks is set to be 64, 128, 256, 512 for 4 residual blocks in the increasing order of depth.

E.1.3 Network Architecture for g_ϕ

For the attenuator g_ϕ , we use a 3-layer MLP with a sigmoid activation at the end to facilitate *forgetting*. To give g_ϕ more view on information of optimization, we concatenate layer-wise mean of gradients and layer-wise mean of weights and feed it into the network. For 4-layer CNN and ResNet-12 in classification, and MLPs in regression and reinforcement learning experiments, the numbers of hidden units are $2l$, $2l$, and l , l is the number of layers of the network.

As for LEO, the case is a bit different because they perform one adaptation in latent codes and one on decoded classifier weights. Thus, we introduce two 3-layer MLPs, one for each. Again, for each MLP, the numbers of hidden units are $2n$, $2n$, and n , where n is the dimension of latent codes or the number of classifier weights.

E.2 Regression

The details of the few shot regression experiments are listed in Table I.

Table I: Implementation detail of regression learning experiments.

Hyperparameter	
policy network	2 hidden layers of size 40 with ReLU
training iterations	50000 epochs
inner update α	0.01
meta update optimizer	Adam
meta batch size	4
k shot	[5,10,20]
loss function	MSE loss
evals	randomly sample 100 sine curves, sample 100 examples (repeated 100 times)

E.3 Reinforcement Learning

The details of the Reinforcement Learning experiments are listed in Table J.

Table J: Implementation detail of reinforcement learning experiments.

Hyperparameter	
policy network	2 hidden layers of size 100 with ReLU
Inner update	vanilla policy gradient
Inner update α	0.01
meta-optimizer	TRPO
training iterations	500 epochs, choose best model
MuJoCo horizon	200
MuJoCo batch size	40
MUJoCo evals	update 4 gradient updates, each with 40 samples for a task
2D navigation horizon	100
2D navigation batch size	20
2D navigation evals	update 4 gradient updates, each with 20 samples for a task

E.4 System

All experiments were performed on a single NVIDIA GeForce GTX 1080Ti.